Supporting Information for:

Comprehensively Assessing the Drivers of Future Air Quality in California

Shupeng Zhu[1], Jeremy R. Horne[1], Michael Mac Kinnon[2], G.S. Samuelsen[2], Donald Dabdub[1],

[1] Computational Environmental Sciences Laboratory, University of California, Irvine, CA 92697, USA

[2] Advanced Power and Energy Program, University of California, Irvine, CA 92697, USA

1. TECH emission mitigation design.

Table S1 displays the assumed mitigation measures to achieve the 2030 GHG reductions target of 40% below 1990 levels and Table S2 displays additional (i.e., including 2030) mitigation measures to achieve the 2050 GHG reduction target of 80% below 1990 levels by 2050. As the horizon year of this study is 2035, the assumptions reflect the full implementation of the 2030 measures and the evolution of the energy sectors towards meeting the 2050 measures. In residential and commercial buildings electric and natural gas efficiency gains are assumed, as well as the electrification of space and water heating. In light duty vehicles (LDV), efficiency gains are assumed via new gasoline internal combustion engine (ICE) vehicles averaging 45 miles per gallon (mpg), and through overall reductions in vehicle miles traveled (VMT). Additionally, increases in zero emission vehicle (ZEV) including battery electric vehicles (BEV), plug-in hybrid electric vehicles (PHEV) with 40 mile range, and hydrogen fuel cell electric vehicles (FCEV) are shown in Figure S1. Heavy- and medium-duty vehicles (HDV and MDV) assume replacement of diesel and gasoline reference vehicles with BEV, FCEV, and other alternative technologies including hybrid diesel and compressed natural gas (CNG) vehicles. Similarly, significant growth in electrification of buses occurs to 2050. Electrification is also assumed in other transportation sources including rail, port technologies (ocean going vessels and cargo handling equipment), and harbor craft. Efficiency measures achieve emission reductions in the industrial sector overall, with higher assumed reductions in the petroleum refining and oil and gas extraction sectors.

The criteria pollutant reductions assumed for the TECH case are determined for year 2035. For example, efficiency increases in tandem with the assumed displacement of gasoline LDV by BEV, PHEV, and FCEV in the High Electrification case in Figure S1 yield a fleet-wide emission reduction of 67% from 2015 levels for all pollutants excluding brake and tire wear. Similarly, efficiency gains in the industrial sector achieve a 43% reduction in refinery emissions from base levels, with other industrial sectors experiencing a 23% reduction.

Table S1. 2030 GHG mitigation measures assumed in the TECH case corresponding to the High Electrification scenario presented in (Mahone et al., 2018).

Sector	Efficiency	Electrification
Buildings	10% reduction in total building energy demand	91% of building energy is electric
Light Duty Vehicles	12% reduction in per capita LDV miles traveled, New gasoline ICE LDV average 45 mpg	6 million zero emission vehicles (20% of total)
Heavy Duty Vehicles	5-6% reduction in shipping energy demand	10% of HDV are hybrid and alternative fuel (4% BEVs/FCEVs), 32% electrification of buses
Transportation Other	5-6% reduction in shipping, harbor-craft, and aviation energy demand	20% electrification of rail, 27% electrification of ports, 26% electric or hybrid harbor craft
Industrial	20% reduction in total industrial, non-petroleum sector energy demand, 14% reduction in refinery output	

Table S2. 2050 GHG mitigation measures assumed in the TECH case corresponding to the High Electrification scenario presented in (Mahone et al., 2018).

Sector	Efficiency	Electrification
Buildings	34% reduction in total building energy demand	91% of building energy is electric
Light Duty Vehicles	24% reduction in LDV miles traveled	35 million zero emission vehicles (96% of total)
Heavy Duty Vehicles	5-6% reduction in shipping energy demand	47% of HDV are BEVs/FCEVs), 31% of HDV is hybrid and CNG, 88% electrification of buses
Transportation Other	5-6% reduction in shipping, harbor-craft, and aviation energy demand	75% electrification of rail, 80% electrification of ports, 77% electric or hybrid harbor craft
Industrial	20% reduction in total industrial, non-petroleum sector energy demand, 90% reduction in refinery and oil and gas extraction energy demand	

Table S3. Anthropogenic emission difference in percentage (%) between mitigation scenarios and the baseline (SOx includes SO2 and H2SO4, TOG includes CH4 and all other VOCs).

Scenario	CO	NOx	NH3	SOx	TOG	PM
CARB	-19.6	-49.4	-2.6	-11.3	-7.6	+6.8
TECH	-25.0	-58.7	-5.2	-21.8	-10.2	+3.6

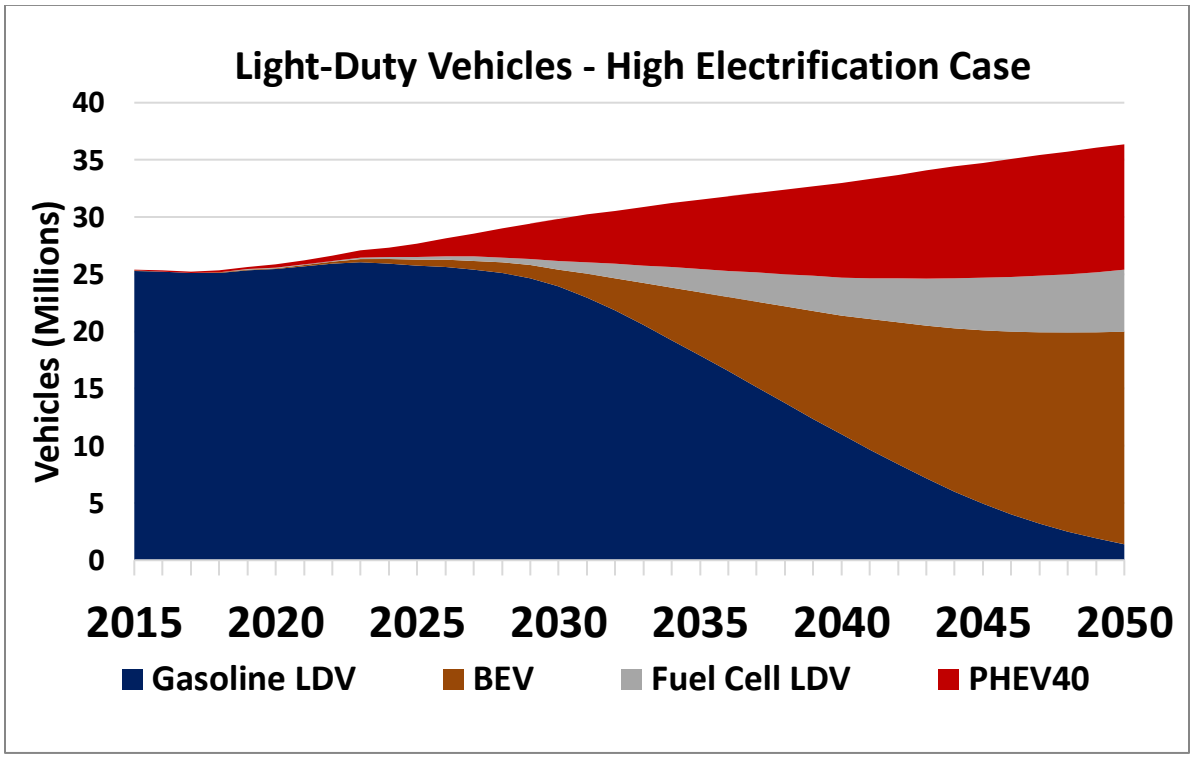

Figure S1. LDV assumed in the High Electrification Scenario in millions. Adapted from PATHWAYS model Transportation and building stock and equipment results at https://www.ethree.com/projects/deep-decarbonization-california-cec/

2. Temporal impact discussion

In general, the temporal variation in pollutant concentrations can be classified into two groups based on overall pattern associated with meteorological conditions. The first group including the BASE, CARB and TECH scenarios (2012 meteorological conditions), and the second group including the MET, CLIM, FUTR-CARB and FUTR+ scenarios (RCP 4.5 2035 meteorological conditions). The classification is relevant for both summer ozone (Figure 3) and winter $PM_{2.5}$ (Figure 5). The distinction between these two groups is clearly visible in Figure 5e for winter $PM_{2.5}$ in SoCAB region, and can also be distinguished in Figure 3e,

Figure 3f and Figure 5f. The two distinct patterns illustrate the dominant impact of metrological condition on the temporal profiles of both ozone and $PM_{2.5}$.

For summer ozone, a general correlation can be found between the temperature profiles and the temporal concentration profiles (see Figure 3a & Figure 3e, and Figure 3b & Figure 3f). In the BASE scenario, spatially averaged MD8h ozone concentrations in the SJV and the SoCAB exceed 70 ppb on numerous days, indicating high ozone concentrations throughout both regions when meteorological conditions are conducive to ozone formation. In the CARB and TECH scenario, when comparing with BASE scenario, higher concentration reductions can be found during high concentration days such as August 8 in Figure 3e and July 12 and August 10 in Figure 3f. In the MET and CLIM scenarios, day-to-day variations in ozone concentrations follow a different pattern than in the base case, reflecting the climate-impacted 2035 meteorological conditions used in these scenarios. Compared with the BASE scenario, the days with the greatest increases in MD8h ozone concentrations days generally coincide with the days that show the greatest temperature increase (e.g., July 26-27 and Aug 22-26). Higher temperatures accelerate photochemical reaction rates, increasing the formation of ozone in these polluted regions. In the comprehensive FUTR-CARB and FUTR+ scenario when all drivers of future air quality are considered simultaneously, their temporal profiles follow a similar trend as MET and CLIM due to the meteorological condition. However, the difference between FUTR-CARB and FUTR+ resembles the difference between CARB and TECH scenarios, only with amplified magnitude. Despite the impact of climate change, MD8h ozone concentrations in the SJV and the SoCAB tend to be lower in the FUTR+ scenario than the BASE scenario on most days during the summer period (Figure 3e & Figure 3f). These decreases in ozone concentrations are due mostly to the significant reductions in anthropogenic precursor emissions of NOx and VOC under the renewable and end-use electrification strategies in the TECH scenario. The importance and effectiveness of controlling anthropogenic precursor emissions in the future is also illustrated by comparing ozone concentrations in the CLIM and FUTR+ scenarios. Thus, reducing anthropogenic emissions may effectively prevent ozone concentrations from increasing in the future if strict emissions control strategies are implemented. However, climate change still shows a penalty to ozone air quality, as illustrated by comparison of the FUTR+ and TECH scenarios. Average ozone concentrations are generally higher in the FUTR+ scenario than in the TECH scenario, indicating that even significant reductions in anthropogenic emissions cannot completely offset climate-driven increases in ozone concentrations.

For the diurnal variation of summer ozone, a clear correlation can be observed between the temperature and the concentration profiles (see Figure 3c & Figure 3g, and Figure 3d & Figure 3h). The ozone concentration increases and decreases as the temperature rises and falls. For the SoCAB, the highest concentration happens between 14:00-15:00 under 2012 meteorological condition (e.g., BASE, CARB and TECH), while it slightly shifts to 15:00-16:00 under the projected climate change effect in 2035 (e.g., MET, CLIM, FUTR-CARB and FUTR+). For the SJV, the highest concentration happens around 17:00 under 2012 meteorological conditions and 16:00 under the projected climate change effect in 2035. The peak also becomes flatter and more symmetric due to climate change in the SJV, while under 2012 meteorological condition the peak is more shifted to the latter hours of the day. These differences also correspond to the change of temperature diurnal pattern in the SJV (Figure 3d). In general, the diurnal pattern difference between different scenarios is very distinct between the SoCAB and the SJV. In the SoCAB, much larger ozone concentration differences between scenarios can be found during the day than the night, and the difference is most pronounced during peak hours. However, differences

between scenarios are relatively constant throughout the entire day in the SJV, and the largest difference usually happens at night. These results indicate a difference in ozone formation/titration mechanisms that are dominant between the SoCAB and the SJV.

For winter $PM_{2.5}$, the correlation between the temperature and concentration profile is weaker than summer ozone (Figure 5a & Figure 5e, and Figure 5b & Figure 5f). This suggests that climate-driven changes in other meteorological factors such as humidity, mixing height, circulation patterns, and precipitation will strongly influence future PM concentrations. For the BASE scenario, $PM_{2.5}$ concentrations in both the SoCAB and the SJV show significant day-to-day variability, with spatially-averaged concentrations often changing by over 10 µg/m3 on the timescale of a few days. While the SoCAB generally has higher ozone concentrations than the SJV in the summer, $PM_{2.5}$ concentrations in the SJV are typically higher than those in the SoCAB in the winter. In the CARB and TECH scenario, the impact of emission control is much more significant in SJV than in SoCAB. And in general, the greatest reductions in $PM_{2.5}$ concentrations tend to occur on days when $PM_{2.5}$ concentrations are highest. In the MET and CLIM scenario, their temporal profiles are nearly identical, due to the insignificant changes in both biogenic and anthropogenic emissions due to climate change. In the FUTR-CARB and FUTR+ scenarios, daily variations in $PM_{2.5}$ concentrations more closely resemble those in the CLIM and MET scenarios than the BASE, CARB, and TECH scenarios, reflecting the differences in 2035 RCP4.5 meteorology versus 2012 meteorology.

For the diurnal variation of winter $PM_{2.5}$, a distinct pattern can be found between the SJV and the SoCAB. In the SoCAB, the influence of anthropogenic emissions is clear, with early morning and afternoon peaks in $PM_{2.5}$ concentrations following times of high automobile traffic (Figure 5g). In the SJV (Figure 5h), $PM_{2.5}$ concentrations remain relatively constantly during the early morning until 09:00h, followed by a steady decrease as temperatures rise. In both regions, concentrations increase during the later afternoon hours, although these increases persist into the night only in the SJV. In the CARB and TECH scenarios, the reduction of anthropogenic emissions alters the diurnal profile of $PM_{2.5}$ despite no changes in meteorological conditions from the BASE scenario. The average diurnal profile of $PM_{2.5}$ concentrations in both the SoCAB and the SJV is flattened, with $PM_{2.5}$ concentrations showing less variation throughout the day. In the SoCAB, $PM_{2.5}$ concentrations remain steadier after 09:00h. In the SJV, $PM_{2.5}$ concentrations decrease less during the late morning and afternoon hours and remain steady in the evening and at night rather than increasing. In the MET and CLIM scenarios, although $PM_{2.5}$ concentrations in the SJV are higher on some days compares to the BASE scenario, Figure 5h shows that the overall impact of climate change is to reduce $PM_{2.5}$ concentrations throughout the day in the SJV. Conversely, $PM_{2.5}$ concentrations in the SoCAB are generally higher in the CLIM and MET scenarios than in the BASE scenario, and Figure 5g shows that average $PM_{2.5}$ concentrations remain higher throughout the day. Interestingly, changes in anthropogenic emissions appears to have a larger impact on the shape of the average diurnal profile of winter $PM_{2.5}$ than climate change, particularly in the SoCAB. In the FUTR-CARB and FUTR+ scenarios, hourly wintertime $PM_{2.5}$ concentrations are projected to be lower on average in the future due to a combination of climate-driven changes in meteorological conditions and anthropogenic emissions controls in the SJV. In fact, average hourly $PM_{2.5}$ concentrations in the SJV are lowest in the FUTR+ scenario of all scenarios considered, and concentrations tend to remain relevantly constant throughout the day (Figure 5h). While both climate change and anthropogenic emissions reductions tend to decrease $PM_{2.5}$ concentrations in the SJV, these drivers of future air quality have opposite effects in the SoCAB. In this region, the impact of climate change offsets the reductions in $PM_{2.5}$

that occur in response to emissions reductions, causing $PM_{2.5}$ concentrations to increase in the FUTR-CARB scenario. Additional anthropogenic emissions controls in the FUTR+ scenario offset most of the negative impacts of climate change, although $PM_{2.5}$ concentrations are projected to be higher on average during the afternoon hours. Figure 5e shows that both the frequency and severity of pollution periods may increase in this region in the future, causing sharp changes in $PM_{2.5}$ concentrations over timescales of just a few days. Overall, results indicate that controlling anthropogenic emissions in the future can reduce the severity of these pollution periods but is unlikely to completely offset the negative impact of climate change in the SoCAB.

3. Other Figures and Tables

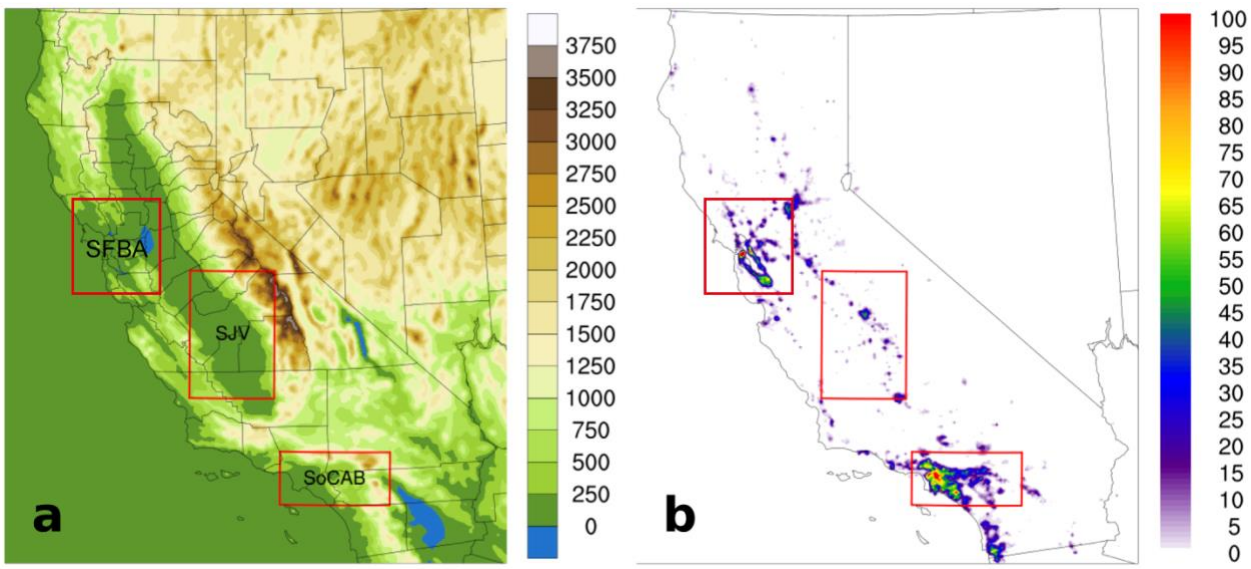

Figure S2: (a) Map of the CMAQ simulation domain showing the three subdomains: San Francisco Bay Area (SFBA), San Joaquin Valley (SJV) and South Coast Air Basin of California (SoCAB). Distance above sea level indicated in meters. (b) Population in each model grid cell in thousands.

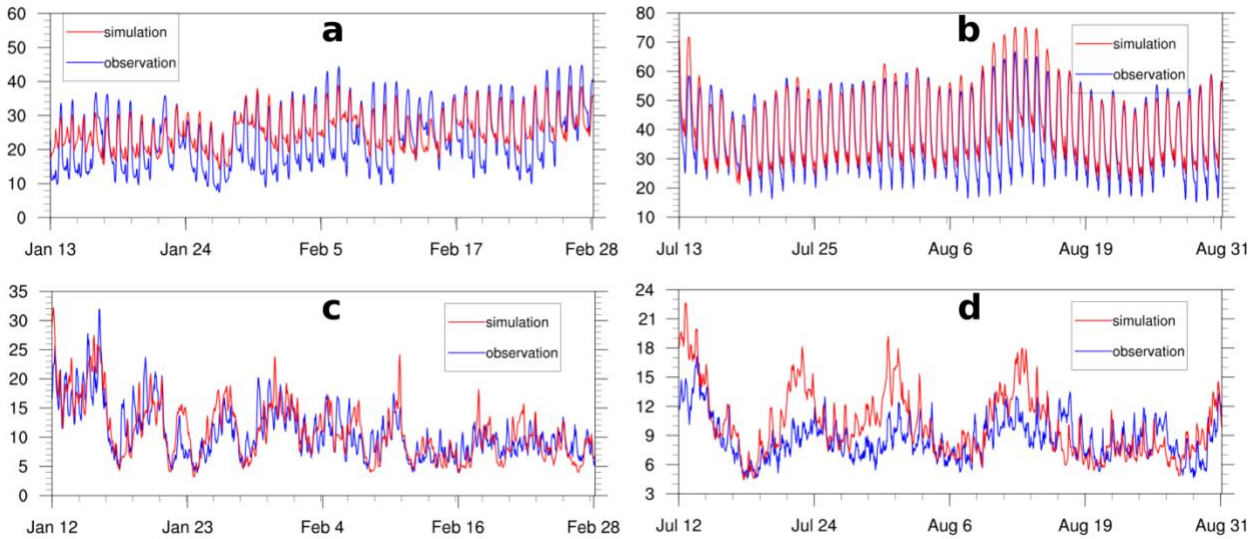

Figure S3: Simulated and Observed hourly ozone (ppb) and $PM_{2.5}$ ($\mu g/m^3$) concentrations for all observation sites in the model domain: (a) Winter ozone, (b) Summer Ozone, (c) Winter $PM_{2.5}$, and (d) Summer $PM_{2.5}$.

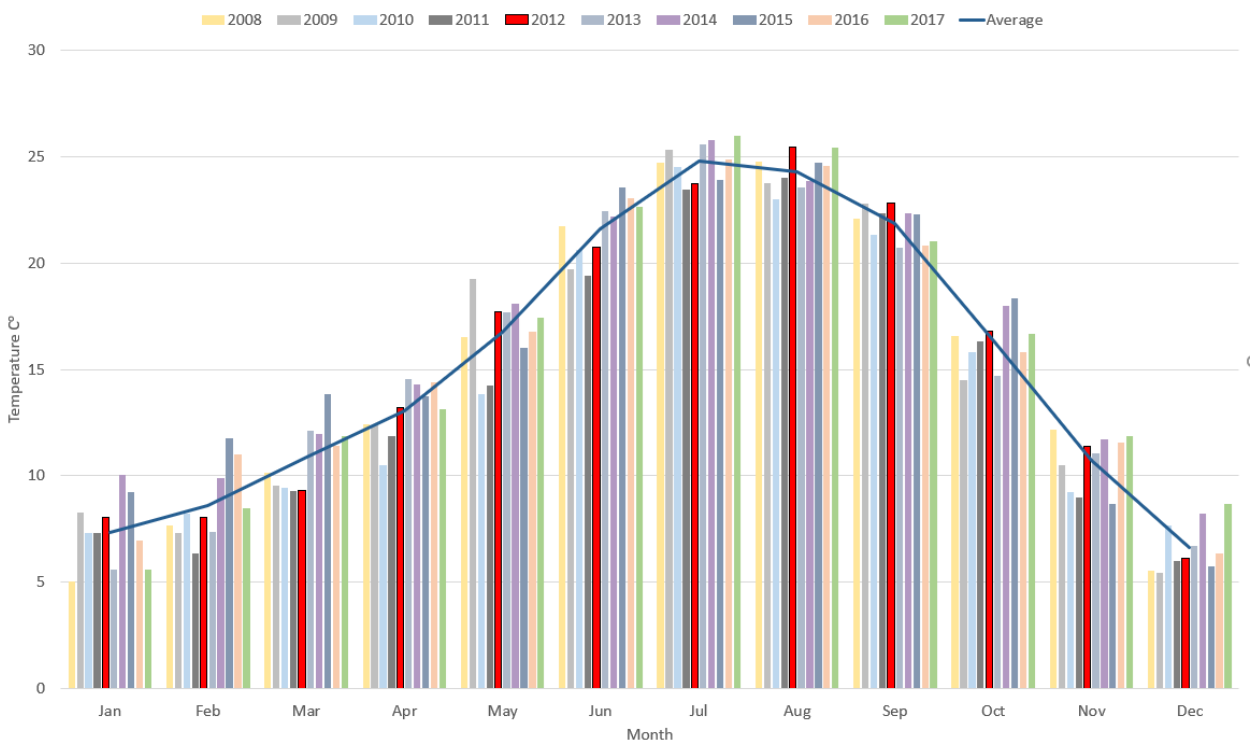

Figure S4: Monthly statewide averaged temperature in California from 2008 to 2017 (Source of data: NOAA https://www.ncdc.noaa.gov/temp-and-precip/).

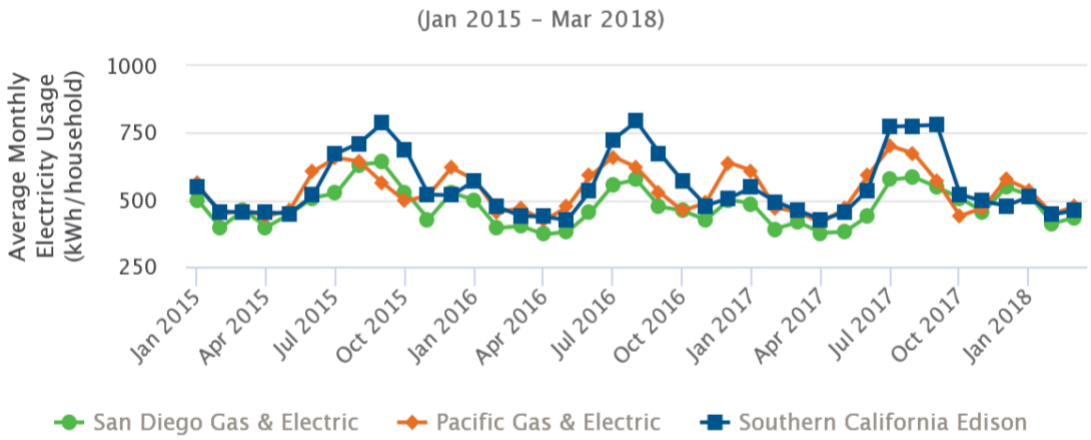

Figure S5. Monthly residential electricity usage in recent three years from the three major electricity providers in California. (Source of data: https://energycenter.org/equinox/dashboard/residential-electricity-consumption)

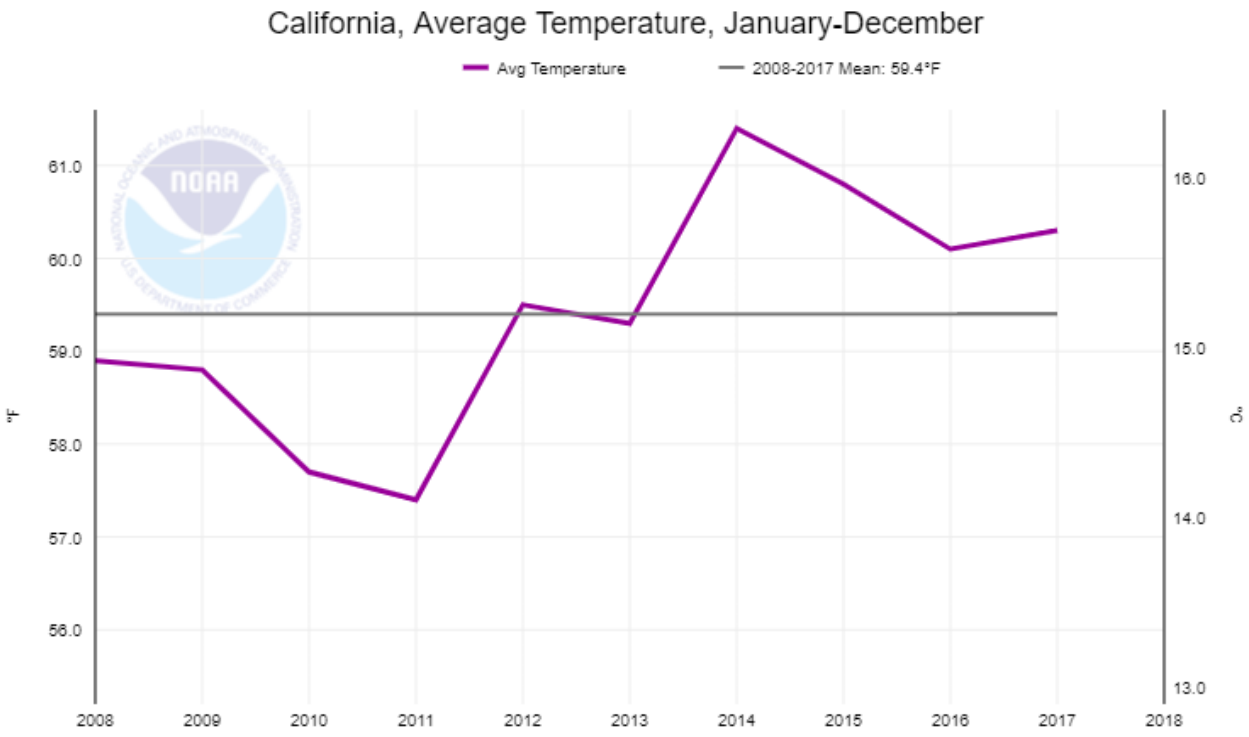

Figure S6: Annual Averaged temperature in California between 2008 to 2017 (Source of data: NOAA https://www.ncdc.noaa.gov/temp-and-precip/).

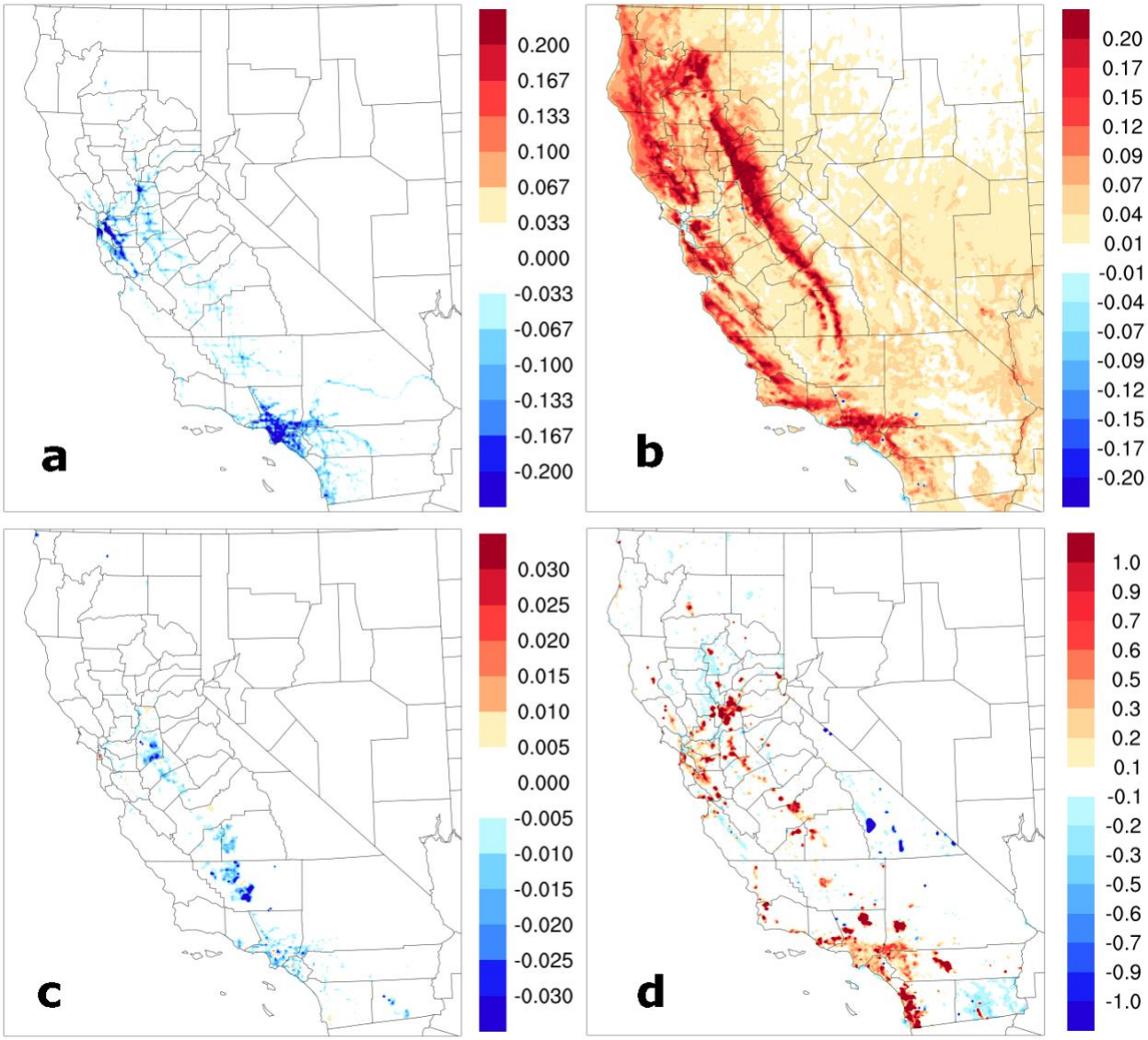

Figure S7: Average changes in emissions of (a) NO_X (moles/s), (b) VOCs (moles/s), (c) NH_3 (moles/s), and (d) $PM_{2.5}$ (g/s) during the summer episode: FUTR+ scenario versus BASE scenario. Positive values represent increases in emissions.

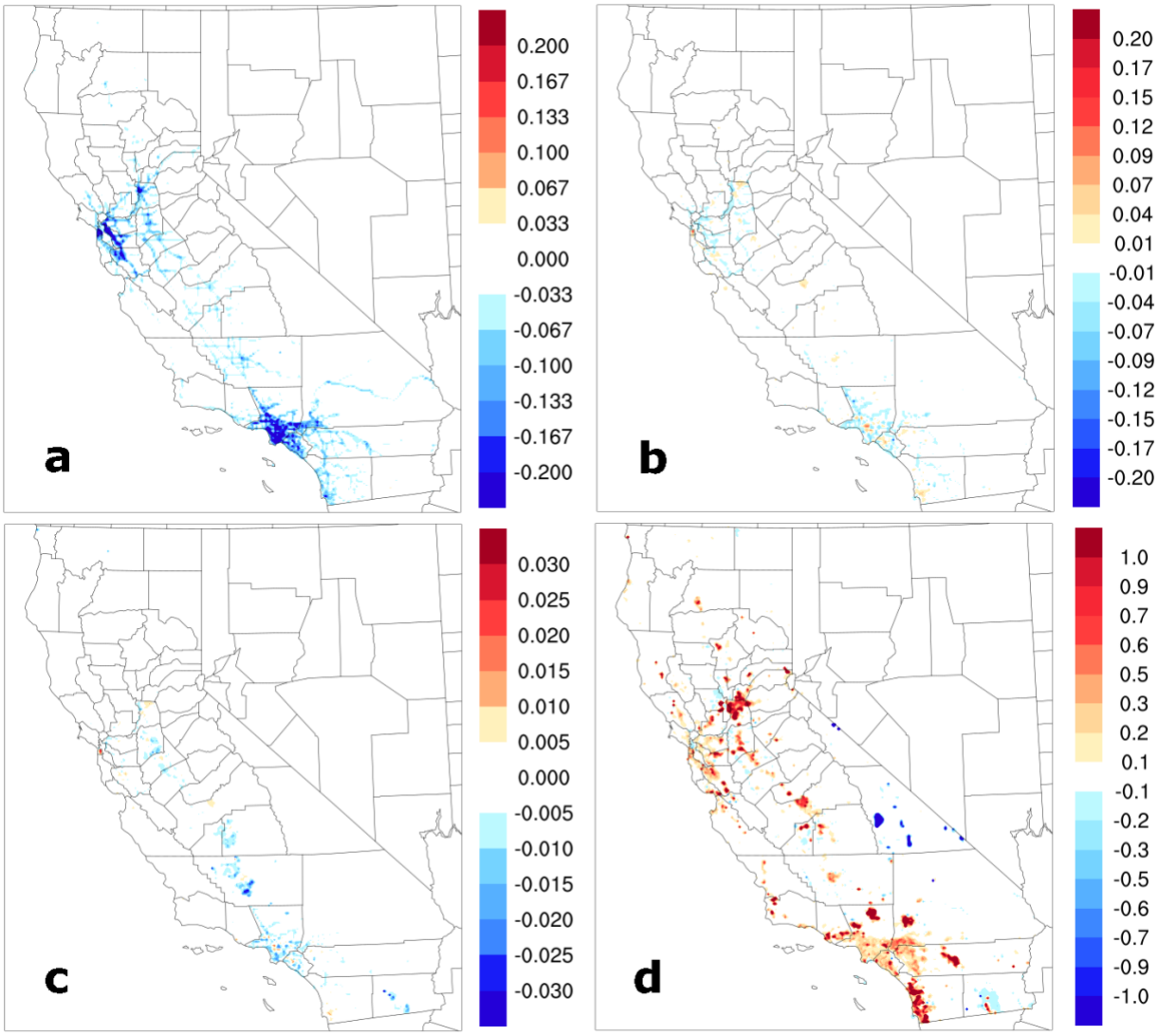

Figure S8: Average changes in emissions of (a) NO_X (moles/s), (b) VOCs (moles/s), (c) NH_3 (moles/s), and (d) $PM_{2.5}$ (g/s) during the winter episode: FUTR+ scenario versus BASE scenario. Positive values represent increases in emissions.

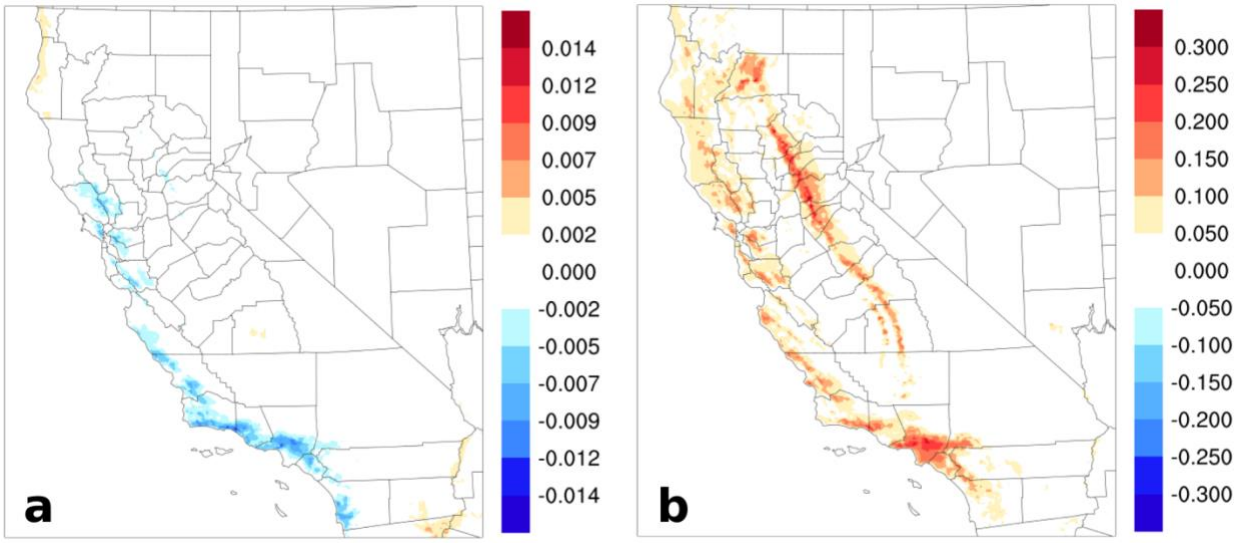

Figure S9: Average difference in biogenic VOC emissions (moles/sec) in the (a) Winter episode and (b) Summer episode: 2035 RCP4.5 meteorolgy versus 2012 baseline meteorology. Positive values indicate increases in biogenic VOC emissions in future years.

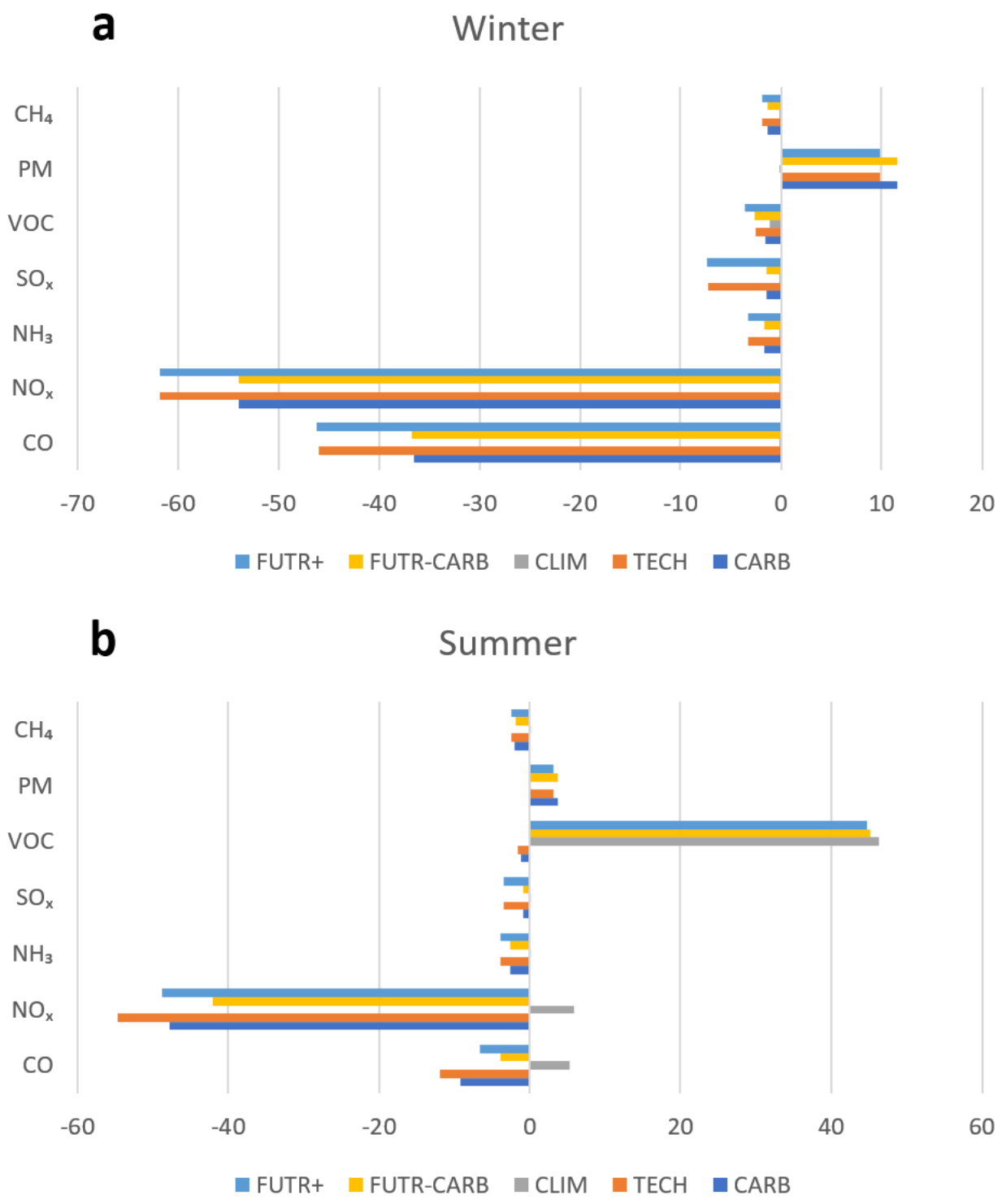

Figure S10: Emission changes in percentage (%) between controlled scenarios and the baseline for both (a) winter and (b) summer period. Note VOC here are without CH_4.

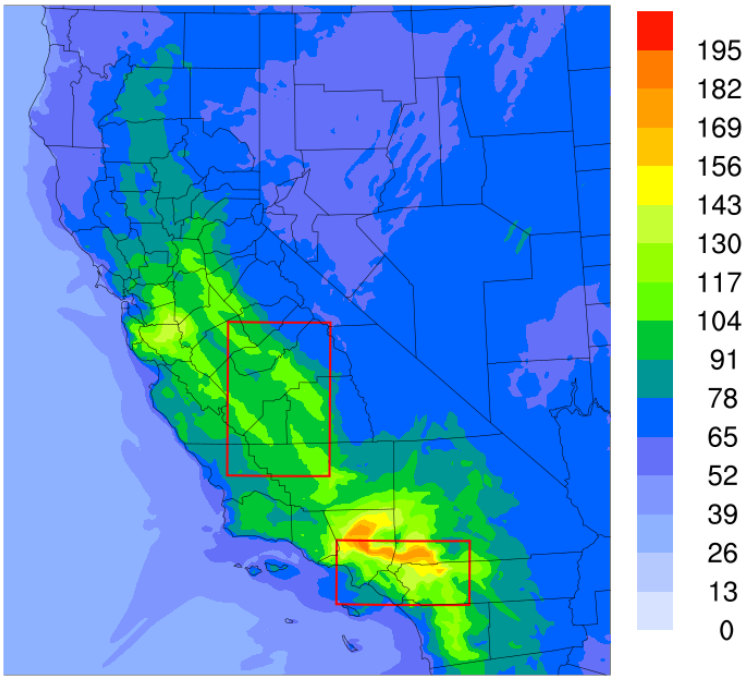

Figure S11: Peak MD8h ozone concentrations (ppb) during the summer period in the MET scenario.

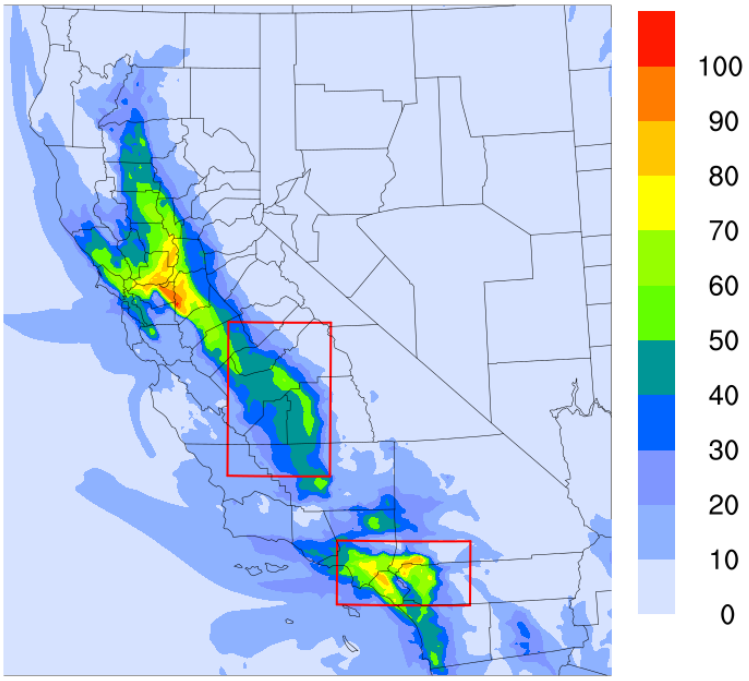

Figure S12: Peak 24-hour average $PM_{2.5}$ concentrations ($\mu g/m^3$) during the winter period in the MET scenario.

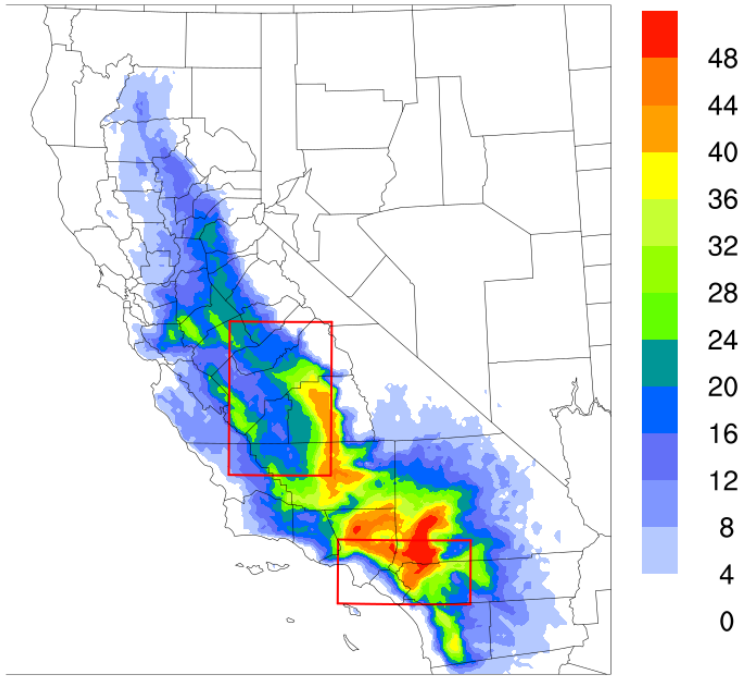

Figure S13**:** The number of days the 70 ppb MD8h ozone standard is exceeded during the summer period in the MET scenario.

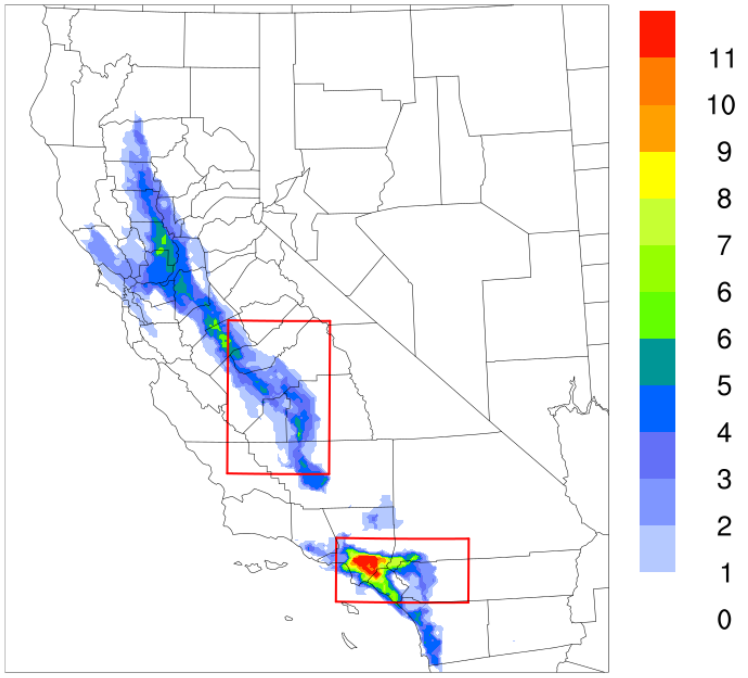

Figure S14: The number of days the 24-hour average 35 µg/m3 **$PM_{2.5}$** air quality standard is exceeded during the winter period in the MET scenario.

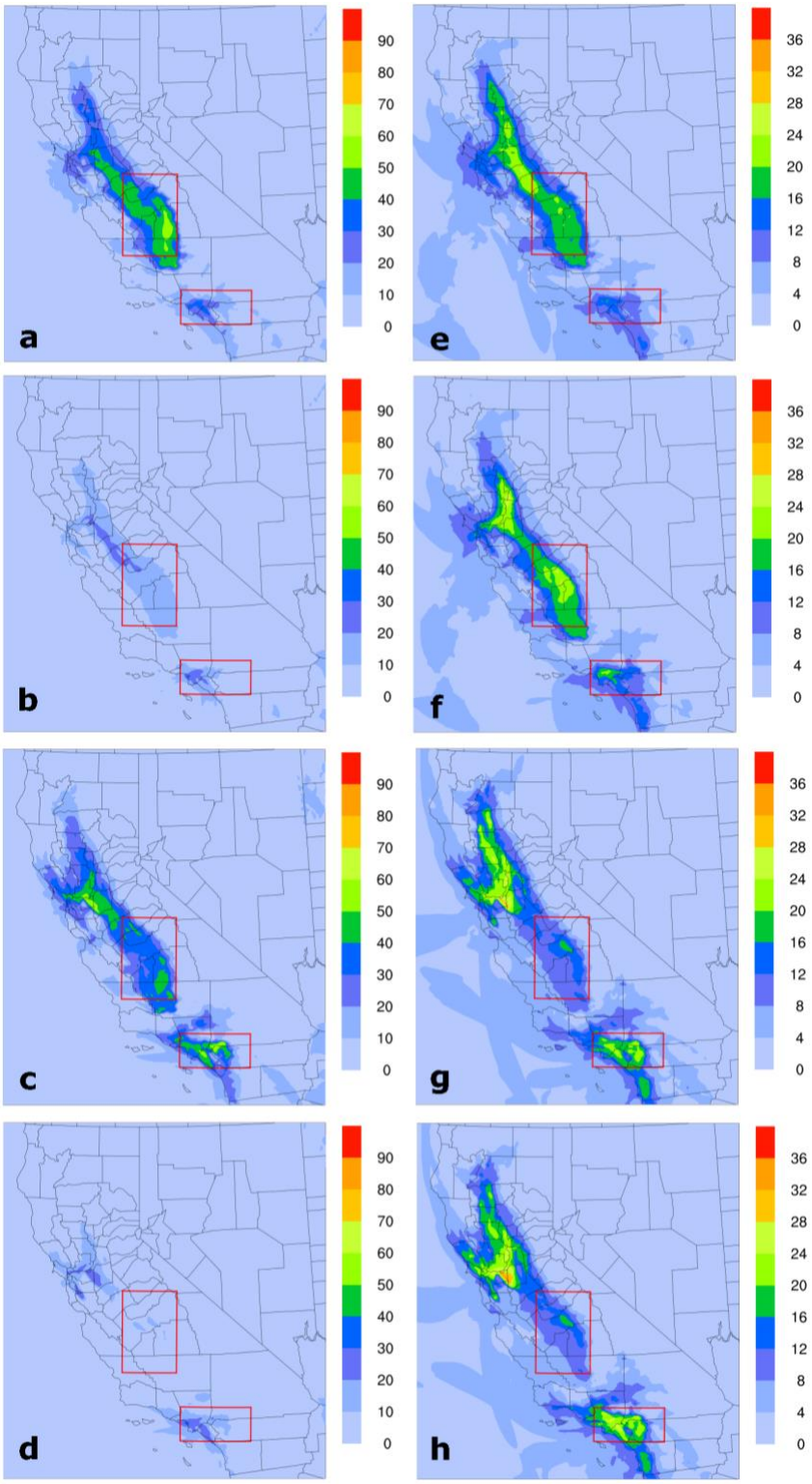

Figure S15: Comparison of inorganic (left column) and organic (right column) $PM_{2.5}$ concentrations. Peak 24-hour average $PM_{2.5}$ concentrations (μg/m^3) of ammonium sulfate (NH_4SO_4) plus ammonium nitrate (NH_4NO_3) in the (a) BASE scenario, (b) CARB scenario, (c) CLIM scenario, and (d) FUTR+ scenario. Peak 24-hour average concentration (μg/m^3) of total organic $PM_{2.5}$ in the (e) BASE scenario, (f) CARB scenario, (g) CLIM scenario, and (h) FUTR+ scenario.

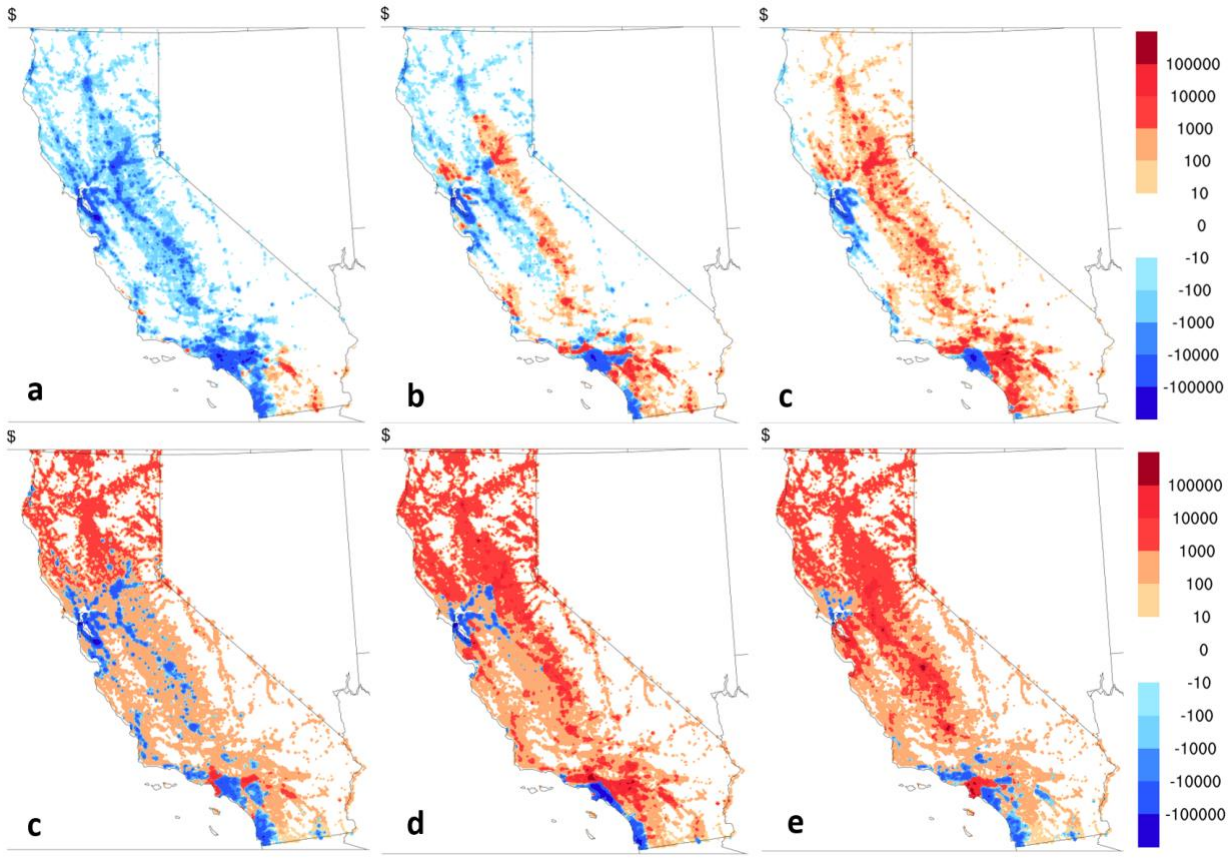

Figure 16. Total health benefit valuation for summer Ozone for (a) CLIM scenario, (b) FUTR-CARB scenario, (c) FUTR+ scenario. Total health benefit valuation for winter $PM_{2.5}$ for (c) CLIM scenario, (d) FUTR-CARB scenario, (e) FUTR+ scenario

Table S4. Definitions of the statistical parameters used in this work. o_i and c_i are the observed and the simulated concentrations at time and location i, respectively. n is the number of data. $\bar{\boldsymbol{o}}$ and $\bar{\boldsymbol{c}}$ are averaged observed and the simulated concentrations, respectively.

Statistic indicator	**Definition**
Root mean square error (RMSE)	$\sqrt{\frac{1}{n}\sum_{i=1}^{n}(c_i - o_i)^2}$
Correlation	$\frac{\sum_{i=1}^{n}(c_i - \bar{c})(o_i - \bar{o})}{\sqrt{\sum_{i=1}^{n}(c_i - \bar{c})^2}\sqrt{\sum_{i=1}^{n}(o_i - \bar{o})^2}}$
Normalized mean bias (NMB)	$\frac{\sum_{i=1}^{n}(c_i - o_i)}{\sum_{i=1}^{n} O_i}$
Normalized mean error (NME)	$\frac{\sum_{i=1}^{n}\lvert o_i - c_i\rvert}{\sum_{i=1}^{n} O_i}$

Table S5. Valuation of reduced short-term exposure to ozone and $PM_{2.5}$ in the all se estimated in BenMAP. Valuation estimates in million $ / day.

Endpoint	Valuation Estimates				
	CARB	TECH	CLIM	FUTR-CARB	FUTR+
Premature Deaths Avoided, All Cause					
Short-Term Ozone Exposure (Summer)	26.93	38.05	-53.09	-12.88	9.488
Short-Term $PM_{2.5}$ Exposure (Winter)	25.05	41.40	-33.52	4.29	15.80
Reduced Morbidity Incidence					
Short-Term Ozone Exposure (Summer)	0.727	1.010	-1.553	-0.358	0.272
Short-Term $PM_{2.5}$ Exposure (Winter)	1.061	1.753	-1.471	0.058	0.679

Table S6. Breakdown by endpoint of the reduced morbidity incidences. Valuation estimates in million $ / day. *Pooled from HA, Chronic Lung Disease (less Asthma) (18-64) and HA, All Respiratory (65 or older) ** Days when normal activities are altered due to ailments

Endpoint (Reduced Morbidity Incidence only)	Valuation Estimates				
	CARB	TECH	CLIM	FUTR-CARB	FUTR+
Short-Term Ozone Exposure (Summer)					
Emergency Room Visits, Asthma	0.019	0.027	-0.043	-0.009	0.007
Hospital Admissions (HA), All Respiratory	0.056	0.080	-0.117	-0.031	0.015
Hospital Admissions (HA), Asthma	0.006	0.008	-0.012	-0.003	0.003
Minor Restricted Activity Days**	0.152	0.214	-0.314	-0.079	0.051
School Loss Days, All Cause	0.494	0.682	-1.068	-12.88	0.195
Short-Term $PM_{2.5}$ Exposure (Winter)					
Acute Myocardial Infarction, Nonfatal	0.579	0.967	-0.834	0.021	0.350
Asthma Exacerbation (Wheeze, Cough, Shortness of Breath)	0.005	0.008	-0.006	0.001	0.004
HA, All Cardiovascular (less Myocardial Infarctions)	0.054	0.091	-0.074	0.003	0.034
HA, All Respiratory (less Asthma) *	0.046	0.077	-0.063	0.002	0.028
HA, Ischemic Stroke	0.073	0.123	-0.103	0.002	0.044
HA and ED Visits, Asthma	0.003	0.004	-0.003	0.4e-4	0.002
Lower Respiratory Symptoms	0.003	0.004	-0.003	0.2e-4	0.002
Upper Respiratory Symptoms	0.005	0.008	-0.006	0.001	0.004
Minor Restricted Activity Days**	0.105	0.169	-0.136	0.009	0.075
Work Loss Days	0.188	0.304	-0.242	0.018	0.136

References

Mahone, A., Kahn-Lang, J., Li, V., Ryan, N., Subin, Z., Allen, D., DeMoor, G., Price, S., 2018. Deep Decarbonization in a High Renewables Future: Updated Results from the California PATHWAYS Model. Sacramento, CA.